EARTHQUAKE ENGINEERING AND STRUCTURAL DYNAMICS
Earthquake Engng Struct. Dyn. 2001; **30**:465–484

Unsupervised fuzzy neural network structural active pulse controller

Shih-Lin Hung*,† and C. M. Lai

Department of Civil Engineering, National Chiao Tung University, 1001 Ta Hsueh Road, Hsinchu 300, Taiwan

SUMMARY

Applying active control systems to civil engineering structures subjected to dynamic loading has received increasing interest. This study proposes an active pulse control model, termed unsupervised fuzzy neural network structural active pulse controller (UFN-SAP controller), for controlling civil engineering structures under dynamic loading. The proposed controller combines an unsupervised neural network classification (UNC) model, an unsupervised fuzzy neural network (UFN) reasoning model, and an active pulse control strategy. The UFN-SAP controller minimizes structural cumulative responses during earthquakes by applying active pulse control forces determined via the UFN model based on the clusters, classified through the UNC model, with their corresponding control forces. Herein, we assume that the effect of the pulses on structure is delayed until just before the next sampling time so that the control force can be calculated in time, and applied. The UFN-SAP controller also averts the difficulty of obtaining system parameters for a real structure for the algorithm to allow active structural control. Illustrative examples reveal significant reductions in cumulative structural responses, proving the feasibility of applying the adaptive unsupervised neural network with the fuzzy classification approach to control civil engineering structures under dynamic loading. Copyright © 2001 John Wiley & Sons, Ltd.

KEY WORDS: active pulse control; dynamic loading

INTRODUCTION

Control of civil engineering structures subjected to dynamic loading, such as those attributed to earthquakes, heavy winds and high waves, can be classified into passive and active controls. A passive control system requires no external power source. On the other hand, in an active control system, external power sources control actuator(s) that apply forces to the structure in a prescribed manner. Active control devices are used in civil engineering structures to modify

* Correspondence to: Shih-Lin Hung, Department of Civil Engineering, National Chiao Tung University, 1001 Ta Hsueh Road, Hsinchu 300, Taiwan.
† E-mail: slhung@cc.nctu.edu.tw

Contract/grant sponsor: National Science Council of Republic of China; contract/grant number: NSC 88-2211-E-009-001.

Received 10 December 1999
Revised 27 June 2000
Accepted 19 July 2000

the structural parameters (stiffness and damping), allowing them to respond more favourably to external excitation [1].

The several analytical theories used for active control of civil engineering structures include optimal control, stochastic control, adaptive control, hybrid control and intelligent control [2] Housner *et al*. [3] indicated that the control strategies deemed appropriate for civil engineering structural control should be simple, but robust and fault tolerant. Additionally, such control strategies not need to be an optimal control, and must be implemented. Intelligent control is a promising approach in the application of automatic structure control systems. Several references from the special issues of *Journal of Engineering Mechanics* [2] give a good overview of intelligent control systems.

Fu [4] proposed the concept of intelligent control to enhance and extend the applicability of automatic control systems. Intelligent controllers can be viewed as adaptive or self-organizing systems that learn through interaction with their environment with little *a priori* knowledge. Two main methodologies related to intelligent control have been developed: (1) artificial neural networks (ANNs) and (2) fuzzy logic. ANNs have been used since the 1980s to identify and control structures in the context of structure control. Nikzad and Ghaboussi [5] first applied multi-layered feedforward networks (MFN) to the problem of digital vibration control of mechanical systems. Wen *et al.* [6] used two ANNs: one to predict the structural response subjected to the control force alone, and the other to predict ground accelerations. Yen [7] applied an indirect predictive learning control scheme for control of a large space structure. Meanwhile, Tang [8] described a simple heuristic-based control strategy capable of applying the control force to cancel the system velocity at the preceding time step for an SDOF system. Chen *et al*. [9] used ANNs to identify the structure system and the trained ANNs can model the structural behaviour. Furthermore, Chen *et al.* [10] proposed a BTTNC active structural control model consisting of two neural networks. One is used for representing the structure to be controlled; the other is trained for determining the actions taken to control the structure. Recently, Hung *et al*. [11] presented an active pulse control model, termed the adaptive neural structure active pulse controller (ANSAP controller), to control civil engineering structures under dynamic loading. The controller consists of two sub-networks: the neural emulator network (NEN) and the neural control network (NCN). The NEN network is used as a system identification model to obtain the structural parameters and it is trained off-line. The NCN model is then used to determine the corresponding control force for the structure represented by the NEN model according to measured structure responses. Other related investigations dealing with ANNs applied to control domains can also be presented in the special issues of the *Journal of Engineering Mechanics* [2].

The theory of fuzzy logic theory developed by Zadeh [12] can be used to model imprecision, ambiguity and fuzziness in vague linguistic information. Adeli and Hung [13] developed a fuzzy neural network learning model by integrating an unsupervised fuzzy neural network classification algorithm with a genetic algorithm and an adaptive conjugate gradient neural network learning algorithm, and applied it to the domain of image recognition. Meanwhile, Hung and Jan[14] presented an unsupervised fuzzy neural network (UFN) reasoning model in structural engineering. Recently, Hung and Jan [15] integrated the UFN reasoning model with a supervised learning model, termed integrating fuzzy neural network (IFN) learning model, and applied it to the problem of structural engineering. In the framework of structural control, Casciati and Yao [16] provide an overview of neural and fuzzy techniques for the control of structures. Faravelli and Yao [17] presented guidelines for implementing a fuzzy active control

strategy for civil engineering structures. Other examples of recent research include Furuta *et al.* [18], Yeh *et al.* [19], Sun and Goto [20] and Nagarajaiah [21].

While extending the above research, this work presents a novel fuzzy-ANN active pulse control model, the unsupervised fuzzy neural network structural active pulse (UFN-SAP) controller, to control civil engineering structures under dynamic loading. The proposed model is based on an unsupervised neural network classification (UNC) model [13], an unsupervised fuzzy neural network (UFN) reasoning model [14, 15] and an active pulse control strategy [22]. The proposed control strategy attempts to reduce cumulative structural responses during earthquakes by applying the active pulse control force. The necessary pulse control forces are determined via the UFN model based on the clusters, classified through the UNC model, with their corresponding control forces. These classified clusters with their corresponding control forces are representative of structural dynamic behaviours. The control effectiveness of the UFN-SAP controller is investigated for an SDOF and a 3DOF structure subjected to the EL Centro, Kobe, and Northridge earthquakes.

ACTIVE PULSE CONTROL ALGORITHM

Active control system in civil engineering structures is based on closed-loop control, implying that the structural response is continually monitored and this information is used to continuously modify the applied control forces. Consider a non-linear structural system with n degree of freedom subjected to an external excitation. The equation of motion is written in matrix notation:

$$\mathbf{M}\ddot{\underline{\mathbf{x}}}(t) + \mathbf{C}\dot{\underline{\mathbf{x}}}(t) + \mathbf{K}\underline{\mathbf{x}}(t) = \mathbf{B}_1\underline{\mathbf{u}}(t) + \mathbf{E}_1\underline{\mathbf{w}}(t) \tag{1}$$

where constant matrices $\mathbf{M}$, $\mathbf{C}$ and $\mathbf{K}$ are, respectively, the mass, damping, and stiffness matrices with $n \times n$ entities; $\underline{\mathbf{x}}(t)$ is the n-dimensional displacement vector with respect to the ground; $\underline{\mathbf{u}}(t)$ is the p-dimensional control force vector, $\underline{\mathbf{w}}(t)$ is the q-dimensional external excitation vector and the $n \times p$ matrix $\mathbf{B}_1$ and $n \times q$ matrix $\mathbf{E}_1$ are location matrices that define the locations of the control force and the excitation, respectively. While assuming that the external seismic force and the control force are piecewise-linear and piecewise-constant interpolation functions, respectively, the external seismic force and the control force are expressed in the following forms:

$$\underline{\mathbf{u}}(\tau) = 0, \quad k\Delta t \leqslant \tau < [(k+1)\Delta t - \Delta t_u] \tag{2}$$

$$\underline{\mathbf{u}}(\tau) = \underline{\mathbf{u}}[k\Delta t], \quad [(k+1)\Delta t - \Delta t_u] \leqslant \tau < (k+1)\Delta t \tag{3}$$

$$\underline{\mathbf{w}}(\tau) = \frac{\tau - k\Delta t}{\Delta t}\{\underline{\mathbf{w}}[(k+1)\Delta t] - \underline{\mathbf{w}}[k\Delta t]\} + \underline{\mathbf{w}}[k\Delta t], \quad k\Delta t \leqslant \tau < (k+1)\Delta t \tag{4}$$

where $k = 0, 1, 2, \ldots, N$, is an integer number, Δt is the time length of the sampling period and Δt_u is the time length of applying the control force. Therefore, Equation (1) can be written in a discrete state form as follows:

$$\underline{\mathbf{z}}[k+1] = \mathbf{A}_p\underline{\mathbf{z}}[k] + \mathbf{B}_p\mathbf{B}\underline{\mathbf{u}}[k] + \mathbf{E}_{p1}\mathbf{E}\underline{\mathbf{w}}[k+1] + \mathbf{E}_{p2}\mathbf{E}(\underline{\mathbf{w}}[k+1] - \underline{\mathbf{w}}[k]) \tag{5}$$

where $\mathbf{A}_p = e^{\mathbf{A}\Delta t}$, $\mathbf{B}_p = \mathbf{A}^{-1}(e^{\mathbf{A}\Delta t_u} - \mathbf{I})$, $\mathbf{E}_{p1} = \mathbf{A}^{-1}(\mathbf{A}_p - \mathbf{I})$, $\mathbf{E}_{p2} = \mathbf{A}^{-1}(\mathbf{E}_{p1}/\Delta t - \mathbf{A}_p)$, and

$$\underline{\mathbf{z}}[k+1] = \begin{bmatrix} \underline{\mathbf{x}}[k+1] \\ \dot{\underline{\mathbf{x}}}[k+1] \end{bmatrix}_{2n\times 1}$$

is a $2n$-dimensional state vector of the structure response at time $t = (k+1)\Delta t$. The system matrix $\mathbf{A}$ and location matrices $\mathbf{B}$ and $\mathbf{E}$ can be determined by the following:

$$\mathbf{A} = \begin{bmatrix} \mathbf{0} & \mathbf{I} \\ -\mathbf{M}^{-1}\mathbf{K} & -\mathbf{M}^{-1}\mathbf{C} \end{bmatrix}_{2n\times 2n} \tag{6}$$

$$\mathbf{B} = \begin{bmatrix} \mathbf{0} \\ \mathbf{M}^{-1}\mathbf{B}_1 \end{bmatrix}_{2n\times p} \tag{7}$$

$$\mathbf{E} = \begin{bmatrix} \mathbf{0} \\ \mathbf{M}^{-1}\mathbf{E}_1 \end{bmatrix}_{2n\times q} \tag{8}$$

The first two terms on the right-hand side of Equation (5) represent the structural response at time $k(\Delta t)$ after the active pulse force $\underline{\mathbf{u}}[k]$ has been applied. With applying a pulse control force $\underline{\mathbf{u}}[k]$, the structural response $\underline{\mathbf{z}}[k]$ at any time $k(\Delta t)$ should be eliminated, as $\underline{\mathbf{z}}^*[k] = \mathbf{A}_p\underline{\mathbf{z}}[k] + \mathbf{B}_p\mathbf{B}\underline{\mathbf{u}}[k] = 0$. Then the control force can be obtained by

$$\underline{\mathbf{u}}[k] = -(\mathbf{B}^{\mathrm{T}}\mathbf{B})^{-1}\mathbf{B}^{\mathrm{T}}\mathbf{B}_p^{-1}\mathbf{A}_p\underline{\mathbf{z}}[k] = \mathbf{G}\underline{\mathbf{z}}[k] \tag{9}$$

The matrix $\mathbf{G}$ is called a state feedback gain matrix and equals to

$$\mathbf{G} = -(\mathbf{B}^{\mathrm{T}}\mathbf{B})^{-1}\mathbf{B}^{\mathrm{T}}\mathbf{B}_p^{-1}\mathbf{A}_p \tag{10}$$

Such a control approach is called an active pulse control strategy, in which, the control force is applied to minimize the system response that carries over from the current time step to the next time step [11, 22]. In the active pulse control algorithm, the pulse control force applied to the structure is reduced in a $\Delta t_u (\Delta t_u < \Delta t)$ period. Furthermore, the effect of pulses is assumed to be postponed to just before the next sampling time. Consequently, there is time to calculate the control force, to prepare it during the former $\Delta t - \Delta t_u$ period and to apply it to the structure during the later Δt_u period of each time step Δt.

UNSUPERVISED NEURAL NETWORK CLASSIFICATION (UNC) MODEL

This section briefly reviews the unsupervised neural network classification (UNC) model [13]. Assume there is a set with N training instances, $\mathbf{X} = \{\mathbf{X}_1, \mathbf{X}_2, \ldots, \mathbf{X}_N\}$. Instance $\mathbf{X}_j$ is defined as a pair including input $X_{j,i}$ and its corresponding output $X_{j,\mathrm{o}}$. If there are M decision variables in the input and K data items in the output, then, the input $X_{j,\mathrm{i}}$ and output $X_{j,\mathrm{o}}$ of instance $\mathbf{X}_j$ are represented as vectors of the decision variables and data, and are denoted as $X_{j,i} = [x_j^1, x_j^2, \ldots, x_j^M]$ and $X_{j,\mathrm{o}} = [o_j^1, o_j^2, \ldots, o_j^K]$. The clustering process aims to classify the set of training instances into a certain number of clusters based on predetermined features from the training data. The elements in each cluster are as similar as possible to each other and as dissimilar as possible to those in other clusters. Unsupervised classification is conducted using a topology and weight-change neural network. The number of input nodes is made equal to

the number of input decision variables (M) in each training instance. The number of output nodes is set to equal the number of clusters and it will be determined once the classification process is completed.

A neural network with M input nodes and one output node is first generated and the input vector of the first training instance is presented. Then, the input vector of the succeeding training instance is inputted through the network. The classification of a training instance into an existing cluster or a new cluster is based on the notion of maximum likelihood. The unsupervised classification process can be summarized as follows:

1. Calculate the degree of difference, $\mathrm{diff}(\mathbf{X}_j, \mathbf{C}_k)$, between the input vector of a training instance $\mathbf{X}_j$ and each cluster $\mathbf{C}_k$. The function $\mathrm{diff}(\mathbf{X}_j, \mathbf{C}_k)$ is defined as the square Euclidean distance represented as

$$\mathrm{diff}(\mathbf{X}_j, \mathbf{C}_k) = \sum_{m=1}^{M} \alpha_m (x_j^m - c_k^m)^2, \tag{11}$$

   where α_m denotes predefined weight, and is used to represent the degree of importance for the mth decision variable in the input. The weights α_m are generally set as constant based on the heuristic associated learning problem.
2. Find the smallest degree of difference, $\mathrm{diff}_{\min} = \min\{\mathrm{diff}(\mathbf{X}_j, \mathbf{C}_k),\ k = 1, 2, \ldots, Q\}$, for the training instance and assign the cluster with the value of $\mathrm{diff}_{\min}$ to be active. Term Q denotes the number of classified clusters presently.
3. Compare the value of $\mathrm{diff}_{\min}$ with the predefined threshold value κ. If $\mathrm{diff}_{\min}$ is smaller than κ, the training instance belongs to the cluster with the value of $\mathrm{diff}_{\min}$ and the weights associated with the links are updated using a successive estimation approach [13]. If $\mathrm{diff}_{\min}$ greater than κ, the training instance is classified as a new cluster and the topology of the neural network is altered.

Hereinafter, the set of N training instances is classified into a certain number homogeneous clusters, say P. These P distinct clusters represent a discrete feature set for these N training instances. The workability of these P clusters must be verified before they can be used as a *sample* base of the set. The verification process relies on the concept that the input of any instance $\mathbf{X}_i$ in the set $\mathbf{X}$ can be regenerated by combining these P clusters with an acceptable error, provided these P clusters represent the important features of the set. The verification process is summarized in the following steps:

1. For each training instance $\mathbf{X}_j$, calculate the degree of difference, $\mathrm{diff}(\mathbf{X}_j, \mathbf{C}_k)$, between the input vector of the training instance and each cluster $\mathbf{C}_k$ where $j = 1$–N and $k = 1$–P.
2. Collect similar clusters for instance $\mathbf{X}_j$ such that the $\mathrm{diff}(\mathbf{X}_j, \mathbf{C}_k) \leqslant \kappa$. Meanwhile, set the term s_k as $1 - \mathrm{diff}(\mathbf{X}_j, \mathbf{C}_k)/\kappa$ between 0 and 1.
3. Regenerate the input of instance X_j by combining its similar clusters as $X'_{j,i} = (1/\sum_{s=1}^{S} s_s)(s_1\mathbf{C}_1 + s_2\mathbf{C}_2 + \cdots + s_s\mathbf{C}_s)$ and evaluate the error, Δ_j, between the desired and computed input vectors $X_{j,i}$ and $X'_{j,i}$, $\Delta_j = \sum_{m=1}^{M}(x_j^m - x_j'^m)^2$.
4. Calculate the system error $E = \sum_{j=1}^{N} \Delta_j$, an accumulation of the error for each instance. If the system error is below a predefined level, these P clusters are adequate. Otherwise, the threshold value κ is modified and the classification process of the UNC model is initiated to once again re-classify these N training instances.

After the verification process is completed, the corresponding outputs for each cluster can then be obtained. These P distinct clusters with their corresponding output are then collected as a *sample* base for the set.

UNSUPERVISED FUZZY NEURAL NETWORK (UFN) REASONING MODEL

Assume that $\mathbf{U}$ is an associated sample base with P samples $\mathbf{U}_1, \mathbf{U}_2, \ldots, \mathbf{U}_P$ classified via the above UNC model for the aforementioned instance base $\mathbf{X}$ and $\mathbf{Y}$ is a new instance in the same problem domain. The input $U_{j,\mathrm{i}}$ and output $U_{j,\mathrm{o}}$ of sample $\mathbf{U}_j$ are denoted as $U_{j,i} = [u_j^1, u_j^2, \ldots, u_j^M]$ and $U_{j,\mathrm{o}} = [o_j^1, o_j^2, \ldots, o_j^K]$. Similarly, the new instance $\mathbf{Y}$ can also be defined as a pair, including input Y_i and unsolved output Y_o, respectively. The input Y_i is a set of decision variables, $Y_\mathrm{i} = [y^1, y^2, \ldots, y^M]$. The output Y_o is currently a null vector and can be solved using the unsupervised fuzzy neural network (UFN) reasoning model. [14, 15].

The UFN reasoning model is briefly reviewed as follows. Similar to other neural network learning models, the UFN model must first be trained based on a given sample base. The learning stage in the UFN model just involves two stages: determining weights for each decision variable in the input vector and selecting appropriate working parameters for the fuzzy membership function. For the first stage, the weights α_m are set based on the heuristic associated learning problem. The second stage is more complicated and is implemented as follows. The first step is to determine the degree of difference between any two distinct samples in base $\mathbf{U}$. Therefore, a total of $T = C_2^P = P(P-1)/2$ degree of difference has to be calculated. The predefined square Euclidean distance function in Equation (11) is employed to measure the difference, d_{ij}, between two inputs $U_{i,\mathrm{i}}$ and $U_{j,\mathrm{i}}$ for samples $\mathbf{U}_\mathrm{i}$ and $\mathbf{U}_j$ as $d_{ij} = \mathrm{diff}(U_{i,\mathrm{i}}, U_{j,\mathrm{i}}) = \sum_{m=1}^{M} \alpha_m (u_i^m - u_j^m)^2$. After the values of d_{ij} for all samples in base $\mathbf{U}$ are computed, the average of the sum of d_{ij}, denoted as $\bar{d}_{ij} = \mathrm{avg}(d_{ij}) = \sum_{t=1}^{T} (d_{ij})/T$, can be derived. The second step involves determining the fuzzy membership function. In the UFN reasoning model, a 'similarity' between any two samples is represented using a quasi-Z type membership function defined as

$$\mu_{ij} = f(d_{ij}, R_{\max}, R_{\min}) = \begin{cases} 0 & \text{if } d_{ij} \geqslant R_{\max} \\ \dfrac{R_{\max} R_{\min} - R_{\min} d_{ij}}{(R_{\max} - R_{\min}) d_{ij}} & \text{if } R_{\min} < d_{ij} < R_{\max} \\ 1 & \text{if } d_{ij} \leqslant R_{\min} \end{cases} \tag{12}$$

The working variables $R_{\max}$ and $R_{\min}$ are employed to define the upper and lower bounds of the 'degree of difference'. The lower bound $R_{\min}$ is set to a constant 10^{-5}. The upper bound, however, was set as $R_{\max} = \eta \bar{d}_{ij}$. The term η is a real number between 0 and 1 and was established through trial and error.

After the learning in the UFN model is completed, the new instance $\mathbf{Y}$ can be solved via the UFN reasoning model. The process of the UFN reasoning can be summarized in three steps. The first step involves search for samples that resemble the new instance $\mathbf{Y}$ in the sample base $\mathbf{U}$, and performed through a single-layered laterally connected network with an unsupervised competing algorithm. That is, to collect the similar samples with the degree

of difference, $d_{Yj} = \mathrm{diff}(Y_\mathrm{i}, U_{j,\mathrm{i}}) = \sum_{m=1}^{M} \alpha_m (y^m - u_j^m)^2$, less than $R_{\max}$. The second step entails representing the fuzzy relationships among the new instance and its similar samples using Equation (12).

The final step is to generate the output Y_o vector of instance $\mathbf{Y}$ by synthesizing the outputs of similar samples $S_{k,\mathrm{o}}$ according to their associated fuzzy membership values using the center of gravity (COG) method [14, 15]. Assume that R similar samples are collected. Then, the output Y_o of instance $\mathbf{Y}$ yielded via the COG method is defined as follows:

$$Y_\mathrm{o} = \frac{\sum_{k=1}^{R} \mu_k S_{k,\mathrm{o}}}{\sum_{k=1}^{R} \mu_k} \tag{13}$$

where μ_k represents the membership value for the kth similar sample.

The reasoning process of the UFN depends on determining the degree of similarity between $\mathbf{Y}$ and $\mathbf{U}_j$. Consequently, the UFN reasoning model can generate no solution if the new instance entirely differs from all samples in the sample base. Herein, the output of the new instance is simply set as the output of the sample with the smallest degree of difference.

UFN STRUCTURAL ACTIVE PULSE (UFN-SAP) CONTROLLER

For an SDOF structure with an active control device installed and subjected to an external excitation, the responses (dynamic behaviours) of the structure in each time step are monitored and the required control force for the structure can then be determined through the equation of motion. Herein, the structural response with its corresponding control force in time step $k(\Delta t)$ is denoted as an instance $\mathbf{X}_k$. For the entire time history, say H, of excitation, there are total N $(= H/\Delta t)$ training instances can be obtained and collected as a training set, $\mathbf{X} = \{\mathbf{X}_1, \mathbf{X}_2, \ldots, \mathbf{X}_N\}$.

For the entire time history of external excitation, these N instances may be identical or similar to each other. If some particular instances can be systematically collected from these N instances, the dynamic behaviours of the structure under the given external excitation can be represented by a series of these particular instances. The UNC model is a tool permitting these instances to be systematically classified into a certain number of homogeneous clusters, say P, according to their inputs, relative displacement and velocity data in this study. The feasibility of these P clusters is then verified based on the above-mentioned process. Once the verification process is complete, the corresponding control force for each cluster can be obtained. These P distinct clusters with their corresponding output then gathered as a *sample* base for the SDOF structure.

As the structure is subjected to a new excitation, the structural dynamic response of the structure is monitored at each time step. The required control force can then be obtained via the following steps. First, the monitored structural response is compared with the input of each sample in the sample base. Second, the samples with their degree of differences below a predefined threshold are collected as similar samples. Finally, the corresponding control force in the time step is then calculated via a fuzzy synthesis of the outputs of these similar samples. The aforementioned steps can be performed through the UFN reasoning model.

This work proposes a novel fuzzy-ANN active pulse control model, Unsupervised fuzzy neural network structural active pulse (UFN-SAP) controller, to control civil engineering structures under dynamic loading, and Figure 1 schematically illustrate the model. The proposed model

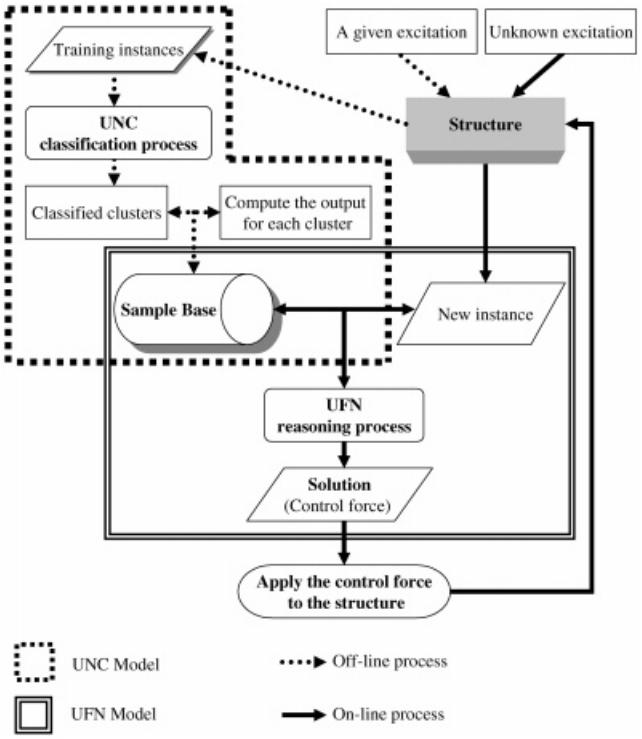

Figure 1. Model of the UFN-SAP controller.

is an integration of a UNC model [13], a UFN reasoning model [14, 15], and an active pulse control strategy [22]. The controller design process is implemented in the following stages. Figure 2 presents a flowchart of these steps.

1. Run a case based on the aforementioned active pulse control algorithm to generate a set of training instances.
2. Classify the set of training instances into a certain number of homogeneous clusters using the UNC model.
3. Verify the feasibility of the classified clusters based on the previously mentioned verification steps.
4. Compute the control force for each cluster and gather it as a sample base for the structure.
5. Train the UFN reasoning model using the sample base.

These stages are off-line design of the UFN-SAP controller. However, applying control force in a structure system is an on-line process. Given a base motion, the response of the structure in each time step is first measured, then the associated control force is determined via the UFN-SAP controller, and finally the control force is applied to the structure to destroy the response of the current time step before the next time step.

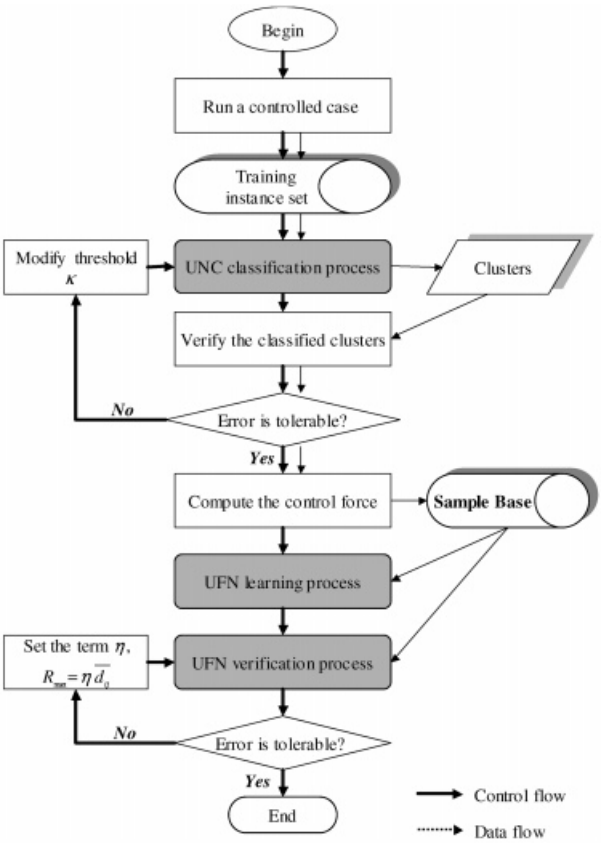

Figure 2. UFN-SAP controller design process.

THE NUMERICAL EXAMPLE

Example 1: SDOF structure system

This section first chooses an SDOF structure system, one-storey structure with an active tendon controller, to explore the control effectiveness of the UFN-SAP controller. This structure is an approximately 1 : 4 scale model of a 1 : 2 scale model of the prototype structure. Table I lists the properties of the SDOF system. The EL-Centro earthquake recorded data (PGA = 0.348g), referred to as Base Motion One, are enlarged to 150 per cent of the original intensity to be used as the greatest external excitation imaginable (0.522g) for the 1 : 4 scale model. The sampling period Δt is 0.01 s. Figure 3 depicts the time history and the corresponding acceleration spectra of base motion one.

Controller design: The response of the SDOF structure is first calculated for base motion one using Equation (5). The pulse duration Δt_u is assumed to be half of the sampling period Δt, i.e. $\Delta t_u = 0.005$ s. Herein, the kth instance is set as $\mathbf{X}_k = \lfloor(\underline{\mathbf{x}}[k], \underline{\dot{\mathbf{x}}}[k]), \underline{\mathbf{u}}[k]\rfloor$. Consequently,

Table I. System parameter values for the SDOF example.

Parameter	Quantity
Mass, m	2923.38 kg
Structure stiffness, k	1391.06 kN m^{-1}
Natural frequency, f_0	3.47 Hz
Damping factor, ζ	5%
Damping coefficient, c	6373.74 N − s m^{-1}

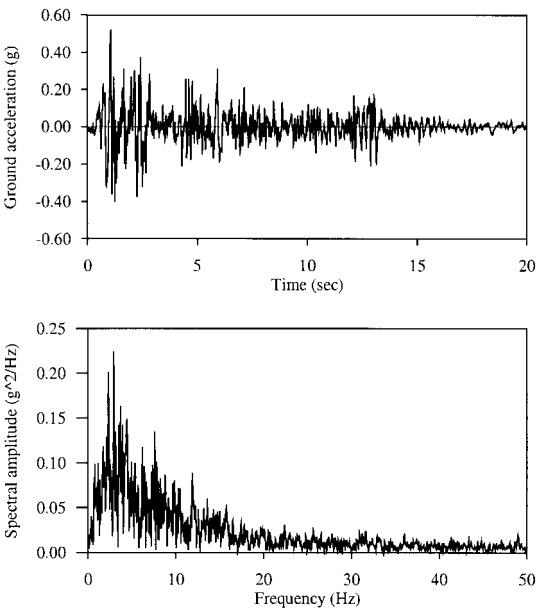

Figure 3. (a) Time history and (b) the acceleration spectrum of base motion one.

2000 instances are obtained for base motion one and the first 1500 instances are taken as training instances for the UNC model. Setting the threshold value, κ, as 0.0012 via trial and error, 127 clusters are classified after the clustering process in the UNC model is completed. The feasibility of these 127 clusters is then verified. The inputs of these 1500 training instances are regenerated using these 127 classified clusters. The average error for each instance equals 0.008 per cent and it is tolerable. Hence, these 127 clusters are feasible for the SDOF structure.

Subsequently, the corresponding control force for each cluster is calculated. Figure 4 depicts the distribution of these clusters and the relationship among the classified clusters and the 1500 training instances. This figure reveals that each training instance is circled to one or more clusters where the radius of each circle (cluster) exactly equals the square root of threshold value κ. Figure 5 also shows the range and distribution of the control forces. According to this figure, these control forces are linearly distributed in the maximum and minimum range.

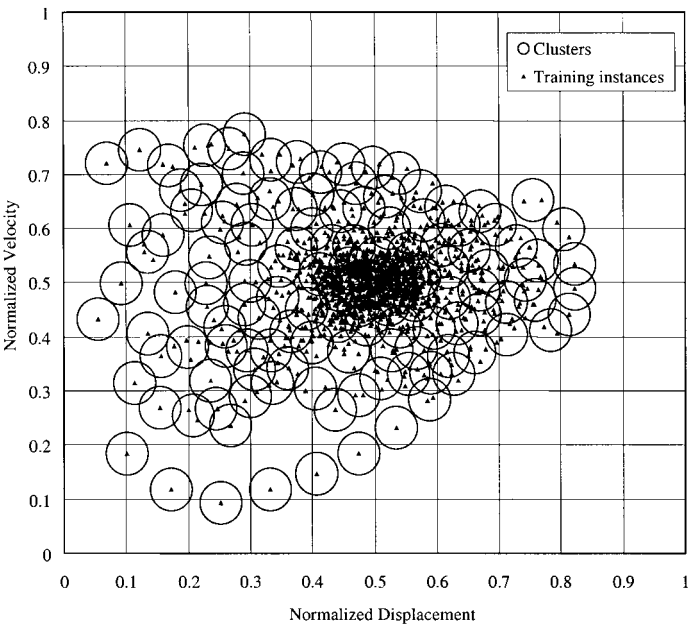

Figure 4. Distribution of the classified clusters and training instances.

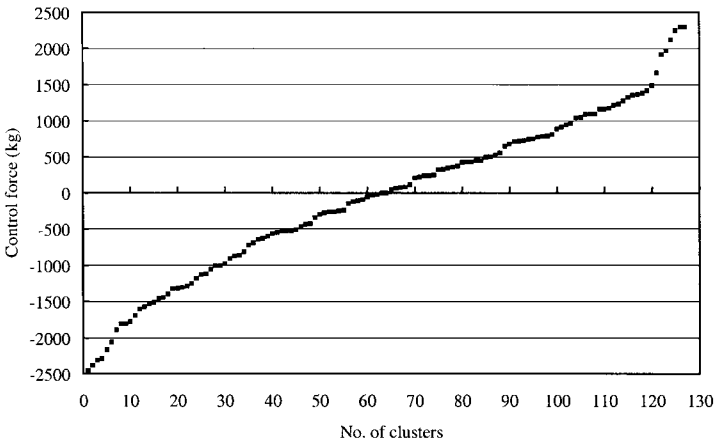

Figure 5. Distribution of the control forces for the clusters.

The UFN reasoning model is trained based on the sample base. A total of 900 instances are used as training instances, including 500 untrained and 400 trained instances randomly selected from the 1500 training instances. The value $\bar{d}_{ij}$ is calculated based on these 900 instances. Setting the term η as 0.8, the value of $R_{\max}$ for the fuzzy membership function in the UFN reasoning model is 0.003. Based on these working parameters, the corresponding control force for each training instance is generated via the UFN reasoning model. For the

Table II. Results for some verification instances: Similar samples associated with the verification instances.

No. of verification instance	No. of similar samples	Input decision variables		Desired output	Computational output	Absolute error	Relative error (%)
		Displacement	Velocity				
12	3,89,90,92	0.47644	0.56195	0.43529	0.43592	0.00063	0.15
50	1,5,6	0.51481	0.46148	0.54028	0.54041	0.00014	0.03
61	1,2,3,89,92,97	0.45976	0.52995	0.46198	0.45619	0.00579	1.25
100	1,4,5	0.54624	0.49857	0.51217	0.51236	0.00020	0.04
105	1,5,6	0.51463	0.44449	0.55647	0.56244	0.00597	1.07
150	1,3,4,92,98	0.49626	0.54101	0.45993	0.45377	0.00616	1.34
200	1,2,3,91,92	0.47652	0.50555	0.48921	0.49180	0.00259	0.53
300	1,2,3,5,91	0.49330	0.49309	0.50504	0.50345	0.00159	0.31
400	1,2,3,4,5,92	0.49475	0.50859	0.49057	0.49707	0.00651	1.33
450	1,3,4,5	0.52043	0.49968	0.50508	0.50233	0.00275	0.55
509	25,75,76	0.63945	0.30467	0.71926	0.71912	0.00014	0.02
525	68,69	0.40942	0.76716	0.22350	0.23157	0.00807	3.61
539	25,26,76	0.64301	0.22831	0.79308	0.80088	0.00780	0.98
565	74,75	0.67932	0.38123	0.65539	0.64859	0.00680	1.04
570	57,58	0.44587	0.22480	0.75040	0.74223	0.00817	1.09
589	73,74	0.70365	0.42766	0.61670	0.60582	0.01088	1.76
650	5,6	0.54475	0.43925	0.56852	0.56050	0.00801	1.41
750	1,2,5,91	0.48585	0.48320	0.51275	0.50563	0.00712	1.39
789	10,11	0.36103	0.61772	0.35503	0.35447	0.00056	0.16
794	13,14,15,81,100	0.54810	0.72367	0.29745	0.29917	0.00172	0.58
900	1,2,5,6,91	0.49931	0.46027	0.53782	0.53022	0.00760	1.41

900 training instances, the average absolute error equals 0.0047. The error is tolerable and hence the learning process in the UFN reasoning model is terminated. Table II lists similar samples associated with randomly selected instances from the 900 training instances. Two to six similar samples are found for each instance. For example, instances 50 and 105 share the same similar samples: 1, 5 and 6. However, the computed outputs differ, and equal 0.54041 and 0.56244. This is attributed to the fact that the associated fuzzy membership values for these three similar samples differ from each other in instances 50 and 105. Remarkably, the average computing time in the UFN reasoning process for each instance is less than 0.001 s. This finding implies that the required control force in each time step can be calculated in time ($\Delta t - \Delta t_u = 0.005$ s) and applied to the structure.

Structure control with the UFN-SAP controller: Herein, 2000 training instances of the base motion one are used to explore the control effectiveness of the UFN-SAP controller. Figure 6 displays the controlled and uncontrolled relative displacements under base motion one. This figure reveals that the applied control force destroys the gradual rhythmic buildup of the structural responses. Figure 6 also indicates that the controlled structural responses using the UFN-SAP controller and those obtained via the numerical formulas in Equations (5) and (9) are almost identical. Significantly, the results reveal not only the feasibility of the sample base in representing the dynamic behaviour of the structure but also the high accuracy of the process of fuzzy synthesizing in the UFN reasoning model.

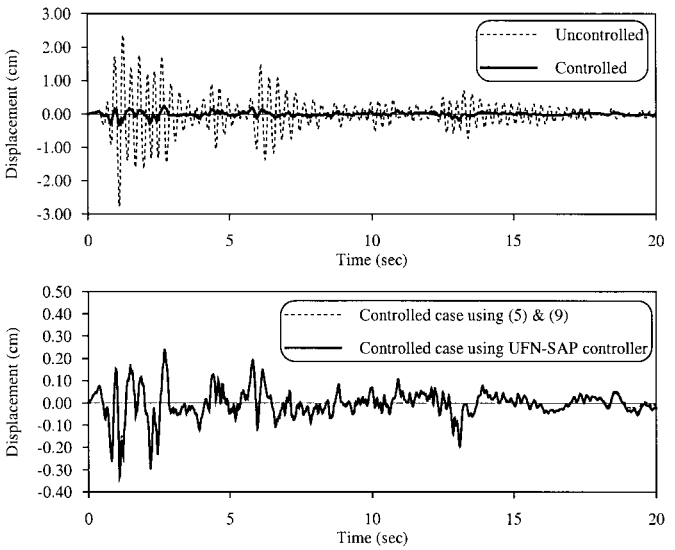

Figure 6. Controlled and uncontrolled relative displacements of the SDOF structure input external excitation: base motion one.

Uncertainty in the input external excitations: Two earthquake recorded data, the Kobe (PGA $= 0.834$g) and Northridge (PGA $= 1.779$g) earthquakes, referred to as base motion two and base motion three, serve as the uncertainty input data, and are scaled to 25 per cent of their original intensity. Figures 7 and 8 display the time history and the corresponding response spectra of base motion two and three, respectively. Herein, base motion two and three are used as external excitation to the SDOF structure.

For the SDOF structure system, base motion two and three are employed as unknown input data. The corresponding control forces are yielded by the UFN-SAP controller based on the 127 samples derived from base motion one. Figure 9 portrays the distribution among the 127 clusters and the instances for base motion two and three. The figure clearly reveals that some instances do not belong to any cluster. In this work, the control forces for these instances approximately equal that of the most similar sample. The results reveal that the responses of the structure are significantly reduced even through the controller design is based on base motion one and there are many differences between the peak, shape, and amplitude of the spectra of base motion one and base motions two and three.

Example 2: 3DOF structure system

A 3DOF structure system is also used to investigate the control effectiveness of the UFN-SAP controller. Notably, the parameters for each floor are identical and assumed to be the same as those of the SDOF structure used in Example 1. Figure 10 depicts the structure with three active tendon controllers installed, respectively, on each floor. This example also uses base motion one to generate the instance set that is then used to train and verify the performance of the UFN-SAP controller. The pulse duration Δt_u is also set as half of the sampling period Δt.

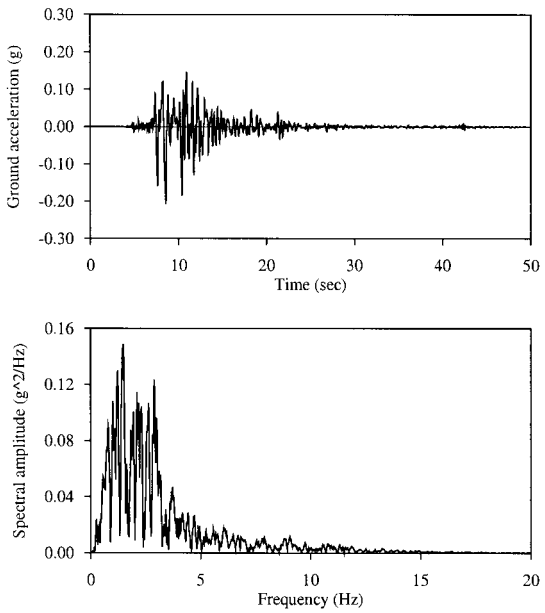

Figure 7. (a) Time history and (b) the acceleration spectrum of base motion two.

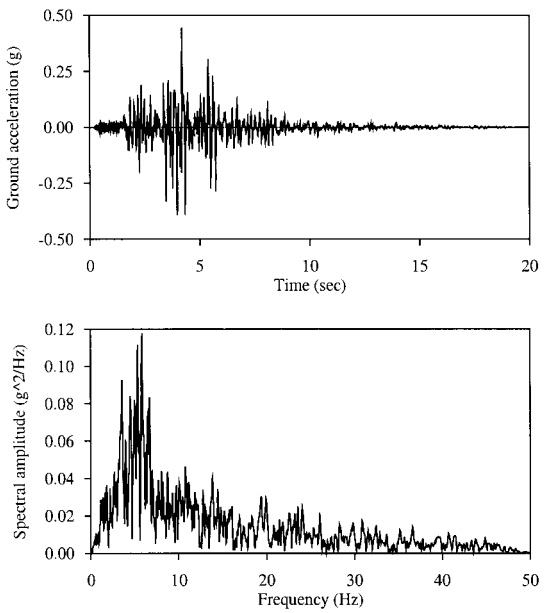

Figure 8. (a) Time history and (b) the acceleration spectrum of base motion three.

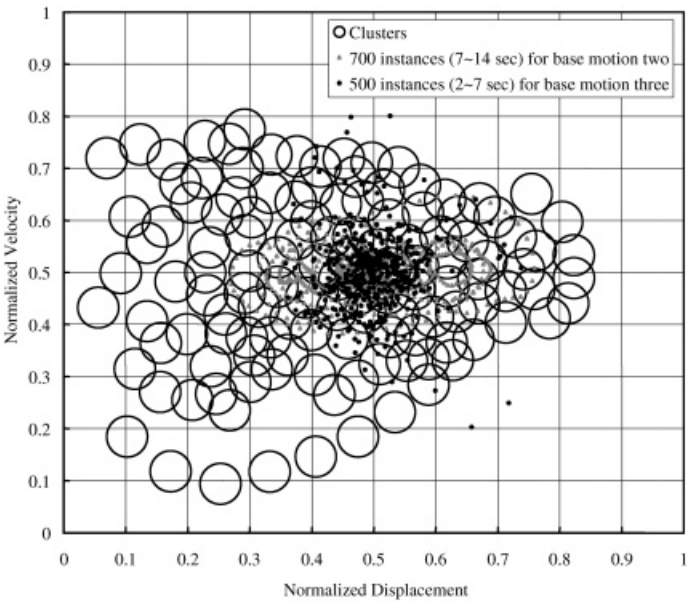

Figure 9. Distribution of the classified clusters and the instances for base motions two and three.

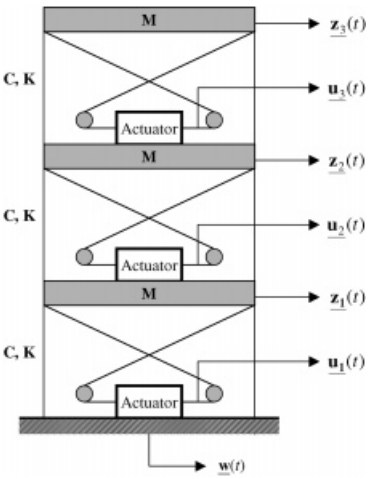

Figure 10. Example of the 3DOF structural system.

Controller design and structure control with the UFN-SAP controller: This example uses the same procedures for designing UFN-SAP controller described in Example 1. However, the response of the structure is the relative displacements and velocities of each floor. That is, a training instance is a pair of inputs (structural responses) and outputs (required control forces), and it is denoted as $\mathbf{X}_k = \lfloor(\underline{\mathbf{x}}_1[k], \dot{\underline{\mathbf{x}}}_1[k], \underline{\mathbf{x}}_2[k], \dot{\underline{\mathbf{x}}}_2[k], \underline{\mathbf{x}}_3[k], \dot{\underline{\mathbf{x}}}_3[k]), (\underline{\mathbf{u}}_1[k], \underline{\mathbf{u}}_2[k], \underline{\mathbf{u}}_3[k])\rfloor$,

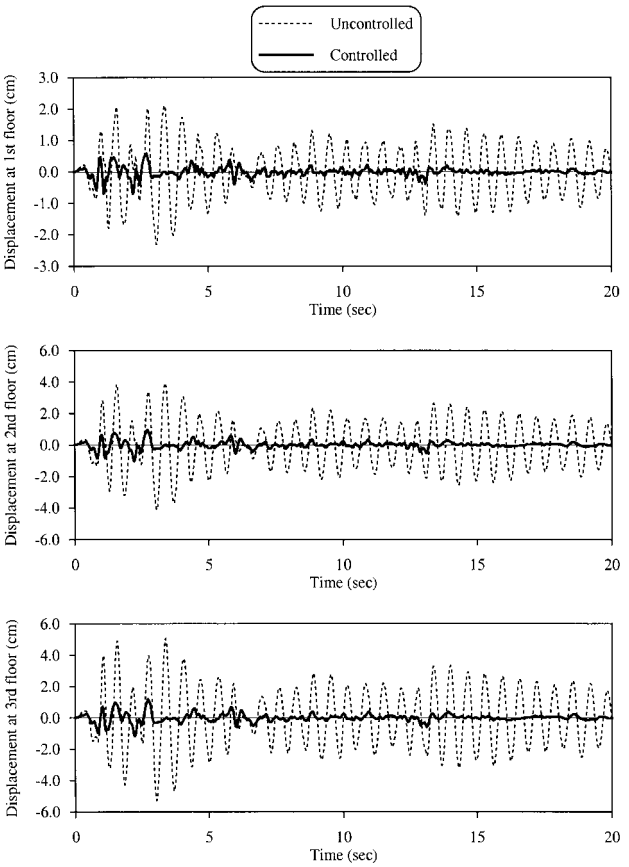

Figure 11. Controlled and uncontrolled relative displacements of the 3DOF structure input external excitation: base motion one.

where the subscripts, 1–3, denote the number of floors. The pair indicates that, at any time step, the required control force in each floor is determined based on the response of each floor at the current time step. Likewise, a total of 2000 instances are obtained based on base motion one and 1500 instances are randomly selected as training instances. The working parameter, κ, for the UNC model is set as 0.0025 through trial and error. The upper bound ($R_{\max}$) of the quasi-Z type membership function in the UFN reasoning model equals 0.006 as the term η is set to 0.8.

Based on these parameters, 269 clusters are first classified through the 1500 training instances using the UNC model. Next, the suitability of these 269 clusters is verified. The average absolute error equals 0.0099 per cent for each training instance and hence is tolerable. Meanwhile, the UFN reasoning model is also trained with the aforementioned parameters. With six input decision variables in each instance, the computing time in the UFN reasoning model for 1500 training instances is about 1 s. That is, the control force can be calculated within the period of ($\Delta t - \Delta t_u$) and then applied to the structure in on-line control. Finally, base motion one is used to investigate the control performance of the UFN-SAP controller.

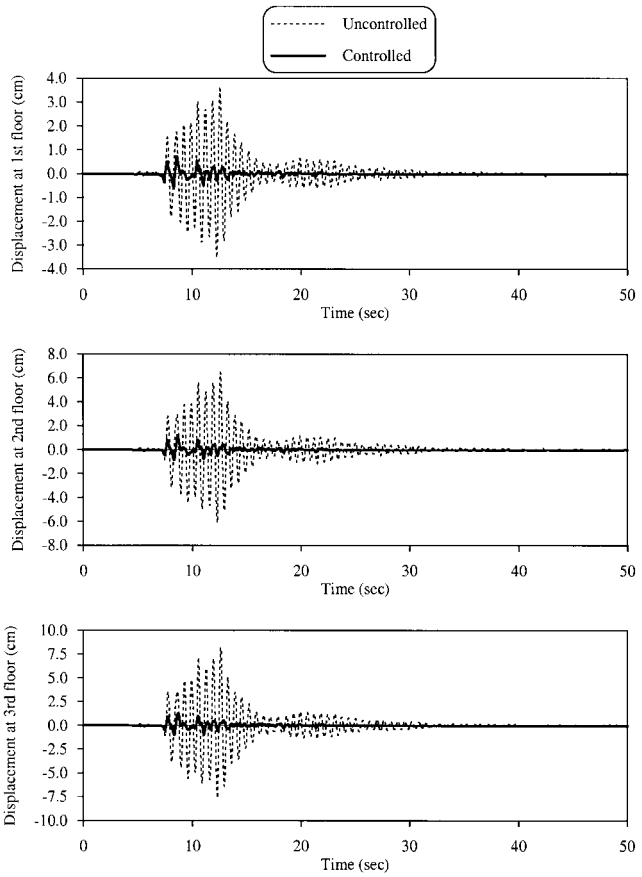

Figure 12. Controlled and uncontrolled relative displacements of the 3DOF structure input external excitation: base motion two.

Figure 11 displays the controlled and uncontrolled displacements for each floor, respectively, of the 3DOF structure system. The results reveal that the structural responses of the structure are significantly reduced.

Uncertainty in the input external excitations: Base motions two and three are also used as the uncertainty input data in this example. The UFN-SAP controller, designed based on the recorded data of base motion one, is used to control the 3DOF structure system under two unknown external excitations. Figures 12 and 13 depict the time history of relative displacements, uncontrolled and controlled, for each floor of the 3DOF structure under base motions two and three, respectively. The figures reveal that the response of the structure is significantly reduced even though the UFN-SAP controller is trained based on the data of base motion one. Table III summarizes the peak values of displacements, uncontrolled and controlled, of the 3DOF structure under three different base motions. The results surely confirm the ability of the UFN-SAP controller to handle uncertain information in the input of external excitations.

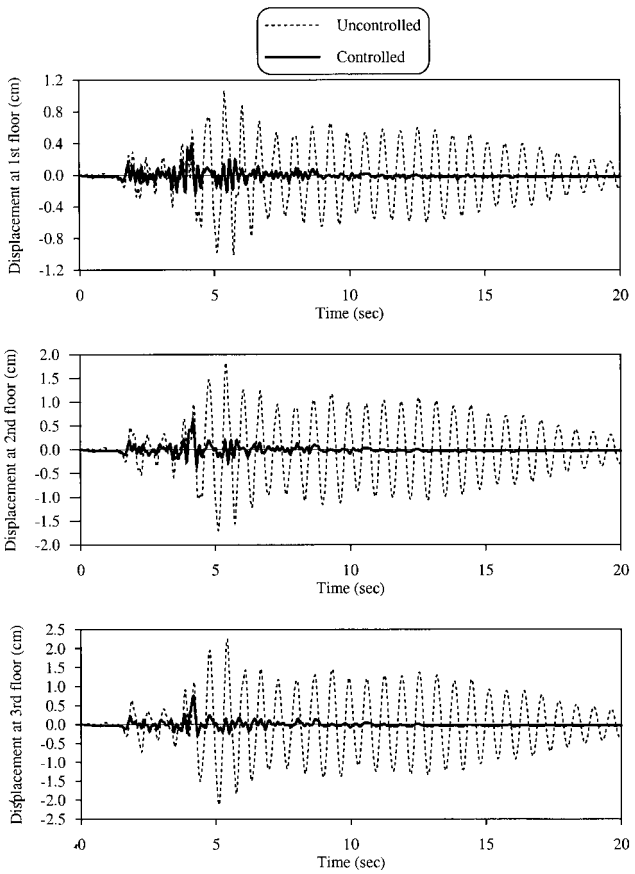

Figure 13. Controlled and uncontrolled relative displacements of the 3DOF structure input external excitation: base motion three.

Table III. Peak values of uncontrolled and controlled relative displacements for different input base motions.

Base motion	Peak values of uncontrolled relative disp. (cm)			Peak values of controlled relative disp. (cm)		
	1st floor	2nd floor	3rd floor	1st floor	2nd floor	3rd floor
One	2.311	4.109	5.282	0.694	1.025	1.163
Two	3.538	6.455	8.137	0.720	1.103	1.274
Three	1.022	1.825	2.238	0.400	0.635	0.757

CONCLUSIONS

This work presented a novel active structure control model, unsupervised fuzzy neural network structure active pulse controller, termed the UFN-SAP Controller, to control structures under

external excitations. The UFN-SAP controller integrates an unsupervised neural network classification (UNC) model [13], an unsupervised fuzzy neural network (UFN) reasoning model [14, 15], and an active pulse control strategy [22]. The pulse control force in the UFN-SAP controller aims to eliminate the cumulative structural responses. For a structure under a given base motion, first, the training instances are obtained using the active pulse control algorithm. Then, these instances are systematically classified into certain number of clusters according to the response of the structure using the UNC model. These clusters with their corresponding control forces are gathered as a sample base. With any unknown base motion, the corresponding control force at each time step for the structure is then derived according the response in the current time step and samples in the sample base using the UFN reasoning model.

Two structure systems, an SDOF and a 3DOF, under three different base motions are used to explore the control effectiveness and capability of handling uncertain input information for the UFN-SAP controller. Examination of the SDOF system reveals that the active control algorithm destroys the gradual rhythmic buildup of the structural response and significantly reduces the structural responses at the peak of the relative displacements. Additionally, the response of the structure are significantly reduced for base motions two and three even the UFN-SAP controller is designed based on the recorder data of base motion one. Remarkably, there are many differences in the peak, shape, and amplitude of the spectra of base motion one and base motions two and three. Meanwhile, a 3DOF structure system with active control device installed in each floor, respectively, demonstrates the control effectiveness and capability of handling unknown input data of the UFN-SAP controller. The results also reveal that the structural responses for each floor are significantly reduced throughout the time history. The UFN-SAP controller is thus clearly useful and extendable to a system with much greater freedoms and non-linear systems.

The control performance of the UFN-SAP controller is heavily dependent on the selection of the working parameter, κ. The smaller κ is, the more clusters can be classified in the instance base, but also the greater the computing time. On the other hand, the larger κ is, the fewer clusters can be derived in the instance base, and these clusters may be insufficient to represent the dynamic behaviour of the structure. This work adopts a heuristic approach to assist the user to obtain an appropriate parameter κ with a minimum of trail-and-error iterations. That is, the distribution of the corresponding control forces for classified clusters will be well-distributed within the range of maximum and minimum values. Meanwhile, the results for the verification process in the UNC model can provide further information for selecting an appropriate parameter κ. A more systematic approach for selecting working parameters is currently being investigated to enhance the effectiveness of the UFN-SAP controller.

ACKNOWLEDGEMENTS

The authors would like to thank the National Science Council of the Republic of China for financially supporting this research under Contract No. NSC 88-2211-E-009-001.

REFERENCES

1. Soong TT. *Active Structural Control*: *Theory and Practice*. Longman Scientific & Technical: Essex, NY, 1990.

2. *Journal of Engineering Mechanics*, Special issue on structure control: past, present, and future. 1997:**123** (September).
3. Housner GW, Soong TT, Masri SF. Second generation of active structural control in civil engineering, final program and abstracts. *First World Conference on Structural Control*, Los Angeles, CA, 3–5, August 1994.
4. Fu KS. Learning control systems and intelligent control systems: an intersection of artificial intelligence and automatic control. *IEEE Transactions on Automatic Control* 1971; **16**: 70–72.
5. Nikzad K, Ghaboussi J. Application of multi-layered feedforward neural networks in digital vibration control. *Proceedings of International Joint Conference on Neural Networks*, Seattle, WA, II A-1004, 1991.
6. Wen YK, Ghaboussi J, Venini P, Nikzad K. Control of structures using neural networks. *Proceedings of US/Italy/Japan Workshop on Structural Control and Intelligent Systems* Sorrento, Italy, 1992; 232–251.
7. Yen GG. Reconfigurable learning control in large space structures. *IEEE Transactions on Control Systems Technology* 1994; **2**(4): 362–371.
8. Tang Y. Active control of SDF systems using artificial neural networks. *Computers and Structures* 1995; **60**(5): 695–673.
9. Chen HM, Qi GZ, Yang JCS, Amini F. Neural network for structural dynamic model identification. *Journal of Engineering Mechanics ASCE* 1995; **121**(12): 1377–1381.
10. Chen HM, Tsai KH, Qi GZ, Yang JCS, Amini F. Neural network for structure control. *Journal of Computers in Civil Engineering ASCE* 1995; **9**(2): 168–176.
11. Hung SL, Lee CJ, Kao CY. Adaptive neural structure active pulse controller. *Proceedings of the IASTED International Conference, Intelligent Systems and Control*, Santa Barbara, CA, U.S.A, October, 28–30 1999; 44–48.
12. Zadeh LA. Fuzzy sets. *Information and Control* 1965; **8**: 338–353.
13. Adeli H, Hung SL. Fuzzy neural network learning model for image recognition. *Integrated Computer-Aided Engineering*, 1993; **1**(1): 43–55.
14. Hung SL, Jan JC. Machine learning in engineering design: an unsupervised fuzzy neural network learning model. *Proceedings of Intelligent Information Systems*, IEEE Computer Society, CA, 1997; 156–160.
15. Hung SL, Jan JC. Machine learning in engineering analysis and design: an integrated fuzzy neural network learning model. *Computer-Aided Civil and Infrastructure Engineering*, 1999; **14**(3): 207–219.
16. Casciati F, Yao T. Comparison of strategies for the active control of civil structures. *Proceedings of 1st World Conference on Structural Control*, WA1, 1994; 3–12.
17. Faravelli F, Yao T. Use of adaptive networks in fuzzy control of civil Structures. *Microcomputers in Civil. Engineering*, 1996; **11**(1): 67–76.
18. Furuta H, Okanan H, Kaneyoshi M, Tanaka H. Application of genetic algorithms to self-tuning of fuzzy active control for structural vibration. *Proceedings of the 1st World Conference on Structural Control*, WA1, 1994; 3–12.
19. Yeh K, Chiang WL, Juang DS. Application of fuzzy control theory in active control of structures. *Proceedings of the First International Industrial Fuzzy Control and Intelligent Systems Conference*, *Fuzzy Information Processing Society Biannual Conference*, *and the NASA Joint Technology Workshop on Neural Networks and Fuzzy Logic*, NAFIPS/IFIS/NASA '94. 1994; 243–247.
20. Sun L, Goto Y. Applications of fuzzy theory to variable dampers for bridge vibration control. *Proceedings of the 1st World Conference on Structural Control*, WP1, 1994; 31–40.
21. Nagarajaiah S. Fuzzy controller for structures with hybrid isolation system. *Proceedings of the 1st World Conference on Structural Control*, TA2, 1994; 67–76.
22. Hung SL, Lee CJ. Neural network for active pulse control of structures. *Proceedings of the Conference on Computer Applications in Civil & Hydralic Engineering*, Hsinchu, Taiwan, R.O.C., 1997; 981–992.

